PROCEEDINGS A

rspa.royalsocietypublishing.org

Research

Cite this article: Clamond D, Dutykh D, Galligo A. 2016 Algebraic method for constructing singular steady solitary waves: a case study. *Proc. R. Soc. A* **472**: 20160194. http://dx.doi.org/10.1098/rspa.2016.0194

Received: 17 March 2016
Accepted: 21 June 2016

Subject Areas:
differential equations, mathematical physics, wave motion

Keywords:
solitary waves, singular solutions, phase plane analysis, algebraic geometry

Author for correspondence:
Didier Clamond
e-mail: didier.clamond@unice.fr

Algebraic method for constructing singular steady solitary waves: a case study

Didier Clamond[1], Denys Dutykh[2] and André Galligo[1]

[1]Université de Nice-Sophia Antipolis, Laboratoire J. A. Dieudonné, Parc Valrose, 06108 Nice Cedex 2, France
[2]Université Savoie Mont Blanc, LAMA UMR-CNRS 5127, Campus Scientifique, 73376 Le Bourget du Lac, France

DC, 0000-0003-0543-8995

This article describes the use of algebraic methods in a phase plane analysis of ordinary differential equations. The method is illustrated by the study of capillary–gravity steady surface waves propagating in shallow water. We consider the (fully nonlinear, weakly dispersive) Serre–Green–Naghdi equation with surface tension, because it provides a tractable model that, at the same time, is not too simple, so interest in the method can be emphasized. In particular, we analyse a special class of solutions, the solitary waves, which play an important role in many fields of physics. In capillary–gravity regime, there are two kinds of localized infinitely smooth travelling wave solutions—solitary waves of elevation and of depression. However, if we allow the solitary waves to have an angular point, then the 'zoology' of solutions becomes much richer, and the main goal of this study is to provide a complete classification of such singular localized solutions using the methods of the *effective* algebraic geometry.

1. Introduction

Ordinary differential equations (ODEs) are the subject of intensive research in mathematics and they play a significant role in all fields where mathematics can be used as a tool to model phenomena (physics, chemistry, biology, economics, etc.). The solutions of ODEs are of special interest in applications because they allow a qualitative description of the phenomenon modelled by the equation. Unfortunately, analytic solutions can rarely be obtained and, most of the time, only numerical solutions are accessible. However, even numerical solutions can be hard to obtain when the equation is

THE ROYAL SOCIETY PUBLISHING

'stiff' [1] or if one is looking for solutions that are not regular. Regular solutions are often the only ones considered in applications, but irregular solutions can also be of special interest. Indeed, such solutions may correspond to physical phenomena (e.g. water waves with angular crest [2]) or to relevant approximations of phenomena (e.g. shock waves). (Here, we are more specifically interested in nonlinear water waves, but it is not a limitation for the purpose of this paper.) Irregular solutions have also been proposed as simple analytical models of regular solutions [3,4] and as elementary basis for numerical approximations such as the finite volumes and finite-elements methods [5,6].

In order to seek exact solutions or to build approximations of an ODE, a qualitative analysis of the equation is very useful. Such analysis can be performed via the so-called *phase plane analysis* (PPA) [7]. The qualitative study of ODEs is an active research field; the first notions of the theory can be found in reference [8]. The main idea here is to extend the usual PPA, thanks to geometrical tools. Instead of a formal abstract description of the method, we find it more enlightening to consider a peculiar example from the physics of nonlinear water waves. Thus, the method is illustrated by the study of capillary–gravity steady surface waves propagating in shallow water. We consider the (fully nonlinear, weakly dispersive) Serre–Green–Naghdi (SGN) equation with surface tension, because it provides a tractable model that, at the same time, is not too simple, so interest in the method can be emphasized.

The general approach to study dynamical systems consists of finding the equilibria first. This part can be done straightforwardly for the SGN system. Our ambition here is to go slightly further and to study the so-called relative equilibria, i.e. steady states in a frame of reference moving with the wave. In the water wave community, they are better known as the *travelling wave* solutions. They can be divided in two distinct classes: the periodic waves and the solitary waves. It will be shown below (see §2d) that the SGN model does not admit any generalized solitary waves, which are connected homoclinically to a periodic wave at infinity. In other words, periodic waves do not interact resonantly with solitary waves in this model. Consequently, as the first attempt, in this paper, we focus only on the case of localized solutions, i.e. the solitary waves. There exists a huge interest in the scientific community to study this particular class of solutions in shallow water-type models, because they might appear as a result of the long-time dynamics stemming from a generic initial condition.

For the SGN-peculiar application, the method results in studying a family of algebraic implicit curves defined in the phase plane. This family depends on two physical parameters (the Froude $\mathscr{F}$ and Bond $\mathscr{B}$ numbers) which characterize the relative importance of inertial, gravity and capillary effects. Depending on the values of these parameters, one can obtain different flow regimes (i.e. sub- or supercritical, for example). For any fixed pair of the parameters $(\mathscr{F}, \mathscr{B})$, our simple PPA provides qualitative results without constructing the exact (analytic or numerical) solutions to the ODE. In this study, we do not limit ourselves to smooth solutions, because the existence of singular solutions to the free surface, Euler equations have been known since the celebrated work of Stokes [2], where he proposed an argument towards the existence of the limiting wave. Later peaked-like solutions have been found in numerous approximate models, such as the Camassa–Holm [9], Degasperis–Procesi [10], just to name a few. Peaked solutions are easily recognizable in the phase plane by symmetric, but discontinuous, paths. For the SGN model, we will be able to find all peakon-like solutions with a vanishing second semi-derivative, the latter condition yielding a zero vertical acceleration at the crest as required by the physics.

The continuous dependence on the parameter values also applies to singular solutions. In other words, a small variation of a generic value of the Froude or Bond numbers (or even both) does not result in any qualitative change of the curve topology in the phase plane as well as in the physical space. The algebraicity of the equations implies that only a finite number of qualitative behaviours (i.e. curve topologies) may appear. By applying the appropriate computer algebraic tools (e.g. resultants and discriminants), we are able to provide the complete classification and description of possible solution behaviours. It should be noted that, in general, algebraic polynomial computations are ill-conditioned in the floating point arithmetics. However, the real

numbers are present in the model only through the Froude and Bond numbers. By keeping these numbers as symbolic parameters, it is possible to perform all the computations in the certified way, which guarantees somehow the qualitative results shown below.

The present manuscript is organized as follows. In §2, we present the simplified ansatz and explain the derivation of the motion equations. In §3, we restrict ourselves to the investigation of steady solitary waves and explain how the problem reduces to the study of a first-order nonlinear differential equation. Then, we consider limiting cases. In §4, we present our PPA techniques. The qualitative properties of the solutions and generalized solutions of the studied differential equation are deduced from algebraic–geometric features of a family of plane curves. In §5, we summarize our work and propose research directions for future investigations.

2. Serre–Green–Naghdi equations with surface tension

In this section, we present briefly the derivation of the SGN equations in the capillary–gravity regime. For long waves in shallow water, the velocity varies little along the vertical, and it is thus mostly horizontal (so-called columnar flows). For such flows, a relevant ansatz fulfilling the incompressibility of the fluid and the bottom impermeability is

$$u(x,y,t)\approx\bar{u}(x,t)\quad\text{and}\quad v(x,y,t)\approx-(y+d)\bar{u}_x, \tag{2.1}$$

where d is the mean water depth and $\bar{u}$ is the horizontal velocity averaged over the water column—i.e. $\bar{u}\equiv h^{-1}\int_{-d}^{\eta}u\,\mathrm{d}y$, $h\equiv\eta+d$ being the total water depth—$y=\eta$ and $y=0$ being the equations of the free surface and of the still water level, respectively.

With the ansatz (2.1), the vertical acceleration is

$$\frac{\mathrm{D}v}{\mathrm{D}t}\equiv\frac{\partial v}{\partial t}+u\frac{\partial v}{\partial x}+v\frac{\partial v}{\partial y}\approx-v\bar{u}_x-(y+d)\frac{\mathrm{D}\bar{u}_x}{\mathrm{D}t}=\gamma\frac{y+d}{h}, \tag{2.2}$$

where γ is the vertical acceleration at the free surface

$$\gamma\equiv\left.\frac{\mathrm{D}v}{\mathrm{D}t}\right|_{y=\eta}\approx h[\bar{u}_x^2-\bar{u}_{xt}-\bar{u}\bar{u}_{xx}]. \tag{2.3}$$

The kinetic $\mathscr{K}$ and the potential energies of gravity $\mathscr{V}_\mathrm{g}$ and capillarity $\mathscr{V}_\mathrm{c}$ are

$$\frac{\mathscr{K}}{\rho}\equiv\int_{t_1}^{t_2}\int_{x_1}^{x_2}\int_{-d}^{\eta}\frac{u^2+v^2}{2}\,\mathrm{d}y\,\mathrm{d}x\,\mathrm{d}t\approx\int_{t_1}^{t_2}\int_{x_1}^{x_2}\left[\frac{h\bar{u}^2}{2}+\frac{h^3\bar{u}_x^2}{6}\right]\mathrm{d}x\,\mathrm{d}t, \tag{2.4}$$

$$\frac{\mathscr{V}_\mathrm{g}}{\rho}\equiv\int_{t_1}^{t_2}\int_{x_1}^{x_2}\int_{-d}^{\eta}g(y+d)\,\mathrm{d}y\,\mathrm{d}x\,\mathrm{d}t=\int_{t_1}^{t_2}\int_{x_1}^{x_2}\frac{gh^2}{2}\,\mathrm{d}x\,\mathrm{d}t \tag{2.5}$$

and

$$\frac{\mathscr{V}_\mathrm{c}}{\rho}\equiv\int_{t_1}^{t_2}\int_{x_1}^{x_2}\tau(\sqrt{1+h_x^2}-1)\,\mathrm{d}x\,\mathrm{d}t, \tag{2.6}$$

where ρ is the (constant) density of the fluid, g is the (constant) acceleration owing to gravity (directed downward) and τ is a (constant) surface tension coefficient (divided by the density). An action integral $\mathscr{S}$ (temporal integral of a Lagrangian) can then be introduced as the kinetic minus the potential energies plus a constraint for the mass conservation (Hamilton principle), i.e.

$$\frac{\mathscr{S}}{\rho}\equiv\int_{t_1}^{t_2}\int_{x_1}^{x_2}\left[\frac{h\bar{u}^2}{2}+\frac{h^3\bar{u}_x^2}{6}-\frac{gh^2}{2}+\tau-\tau\sqrt{1+h_x^2}+\{h_t+[h\bar{u}]_x\}\phi\right]\mathrm{d}x\,\mathrm{d}t, \tag{2.7}$$

where ϕ is a Lagrange multiplier for the term enforcing the mass conservation.

The Euler–Lagrange equations for the functional (2.7) are

$$\delta\phi:\ 0 = h_t + [h\bar{u}]_x, \tag{2.8}$$

$$\delta\bar{u}:\ 0 = \phi h_x - [h\phi]_x - \tfrac{1}{3}[h^3\bar{u}_x]_x + h\bar{u} \tag{2.9}$$

and

$$\delta h:\ 0 = \tfrac{1}{2}\bar{u}^2 + \tfrac{1}{2}h^2\bar{u}_x^2 - gh + \tau[h_x(1+h_x^2)^{-1/2}]_x - \phi_t + \phi\bar{u}_x - [\bar{u}\phi]_x, \tag{2.10}$$

thence

$$\phi_x = \bar{u} - \tfrac{1}{3}h^{-1}[h^3\bar{u}_x]_x \tag{2.11}$$

and

$$\phi_t = \tfrac{1}{2}h^2\bar{u}_x^2 - \tfrac{1}{2}\bar{u}^2 - gh + \tau[h_x(1+h_x^2)^{-1/2}]_x + \tfrac{1}{3}\bar{u}h^{-1}[h^3\bar{u}_x]_x. \tag{2.12}$$

The variable ϕ can be easily eliminated from equations (2.11) and (2.12), and, subsequently, several secondary equations can be obtained. Thus, after some algebra, one gets

$$h_t + [h\bar{u}]_x = 0, \tag{2.13}$$

$$\left[\bar{u} - \frac{(h^3\bar{u}_x)_x}{3h}\right]_t + \left[\frac{\bar{u}^2}{2} + gh - \frac{h^2\bar{u}_x^2}{2} - \frac{\bar{u}(h^3\bar{u}_x)_x}{3h} - \frac{\tau h_{xx}}{(1+h_x^2)^{3/2}}\right]_x = 0, \tag{2.14}$$

$$\left[h\bar{u} - \frac{(h^3\bar{u}_x)_x}{3}\right]_t + \left[h\bar{u}^2 + \frac{gh^2}{2} - \frac{2h^3\bar{u}_x^2}{3} - \frac{h^3\bar{u}\bar{u}_{xx}}{3} - h^2h_x\bar{u}\bar{u}_x - \tau R\right]_x = 0, \tag{2.15}$$

$$[h\bar{u}]_t + \left[h\bar{u}^2 + \frac{1}{2}gh^2 + \frac{1}{3}h^2\gamma - \tau R\right]_x = 0 \tag{2.16}$$

and

$$\left[\frac{h\bar{u}^2}{2} + \frac{h^3\bar{u}_x^2}{6} + \frac{gh^2}{2} + \tau\sqrt{1+h_x^2}\right]_t + \left[\left(\frac{\bar{u}^2}{2} + \frac{h^2\bar{u}_x^2}{6} + gh + \frac{h\gamma}{3} - \frac{\tau h_{xx}}{(1+h_x^2)^{3/2}}\right)h\bar{u} + \frac{\tau h_x(h\bar{u})_x}{(1+h_x^2)^{1/2}}\right]_x = 0, \tag{2.17}$$

where

$$R \equiv hh_{xx}(1+h_x^2)^{-3/2} + (1+h_x^2)^{-1/2}.$$

Physically, these equations characterize the conservations: of the mass (2.13), of the tangential momentum at the free surface (2.14), of the momentum flux (2.15)–(2.16) and of the energy (2.17).

These equations, without surface tension, were first derived by Serre [11], independently rediscovered by Su & Gardner [12], and again by Green *et al.* [13]. These approximations are valid in shallow water without assuming small amplitude waves, so they are sometimes called *weakly dispersive fully nonlinear approximation* [14] and are a generalization of the Saint-Venant and of the Boussinesq equations.

3. Steady waves

The previous equations being Galilean invariant, we consider now a steady wave motion (i.e. a frame of reference moving with the wave where solutions are independent of time). For $2L$-periodic solutions, the mean water depth d and the mean depth-averaged velocity $-c$ are

$$d = \langle h\rangle = \frac{1}{2L}\int_{-L}^{L} h\,\mathrm{d}x \quad \text{and} \quad -cd = \langle h\bar{u}\rangle = \frac{1}{2L}\int_{-L}^{L} h\bar{u}\,\mathrm{d}x, \tag{3.1}$$

thus c is the wave phase velocity observed in the frame of reference without mean flow. The mass conservation (2.13) yields

$$\bar{u} = -\frac{cd}{h}. \tag{3.2}$$

Let $\mathscr{F} = c^2/gd$ be the Froude number squared and let $\mathscr{B} = \tau/gd^2$ be a Bond number; for later convenience, we introduce also the Webber number $\mathscr{W} = \mathscr{B}/\mathscr{F} = \tau/c^2d$. Substitutions of (3.2) into

(2.14) and (2.16), followed by one integration, give

$$\frac{\mathscr{F}d}{h}+\frac{h^2}{2d^2}+\frac{\gamma h^2}{3gd^2}-\frac{\mathscr{B}hh_{xx}}{(1+h_x^2)^{3/2}}-\frac{\mathscr{B}}{(1+h_x^2)^{1/2}}=\mathscr{F}+\frac{1}{2}-\mathscr{B}+\mathscr{K}_1 \tag{3.3}$$

and

$$\frac{\mathscr{F}d^2}{2h^2}+\frac{h}{d}+\frac{\mathscr{F}d^2h_{xx}}{3h}-\frac{\mathscr{F}d^2h_x^2}{6h^2}-\frac{\mathscr{B}dh_{xx}}{(1+h_x^2)^{3/2}}=\frac{\mathscr{F}}{2}+1+\frac{\mathscr{F}\mathscr{K}_2}{2}, \tag{3.4}$$

with

$$\frac{\gamma}{g}=\frac{\mathscr{F}d^3h_{xx}}{h^2}-\frac{\mathscr{F}d^3h_x^2}{h^3},$$

$\mathscr{K}_n$ being dimensionless integration constants to be determined exploiting the conditions (3.1) ($\mathscr{K}_1=\mathscr{K}_2=0$ for solitary waves). Computing (3.3)$-(h/d)\times$ (3.4) in order to eliminate h_{xx} between (3.3) and (3.4), one obtains easily

$$\frac{\mathscr{F}d}{2h}-\frac{h^2}{2d^2}-\frac{\mathscr{F}dh_x^2}{6h}-\frac{\mathscr{B}}{(1+h_x^2)^{1/2}}=\mathscr{F}+\frac{1}{2}-\mathscr{B}+\mathscr{K}_1-\frac{(\mathscr{F}+2+\mathscr{F}\mathscr{K}_2)h}{2d}, \tag{3.5}$$

that is a first-order ODE for h.

The integration constants $\mathscr{K}_n$ are defined from the conditions (3.1). Averaging equations (3.4) and $(d/h)\times$(3.3) yields

$$\mathscr{K}_2=\left\langle\frac{(3+h_x^2)d^2}{3h^2}-1\right\rangle \tag{3.6}$$

and

$$\mathscr{K}_1+\frac{1}{2}+\mathscr{F}-\mathscr{B}=\left\langle\frac{\mathscr{F}d^2}{h^2}+\frac{1}{2}-\frac{\mathscr{B}d/h}{(1+h_x^2)^{1/2}}\right\rangle\Big/\left\langle\frac{d}{h}\right\rangle. \tag{3.7}$$

For infinitesimal periodic waves, we have $h\approx d+a\cos(kx)$ with $|a/d|\ll 1$, thence $\mathscr{K}_1\approx\mathscr{K}_2\approx 0$ and the linearized dispersion relation $\mathscr{F}\approx[1+\mathscr{B}(kd)^2]/[1+(kd)^2/3]$ is obtained.

(a) Solitary waves

Considering solitary waves—i.e. $h(\infty)=d$ thence $\mathscr{K}_1=\mathscr{K}_2=0$—and writing $h'=\mathrm{d}h(x)/\mathrm{d}x$, equation (3.5) multiplied by $(-2h/d)$ becomes

$$F(h',h)\equiv\frac{\mathscr{F}h'^2}{3}+\frac{2\mathscr{B}h/d}{(1+h'^2)^{1/2}}-\mathscr{F}+\frac{(2\mathscr{F}+1-2\mathscr{B})h}{d}-\frac{(\mathscr{F}+2)h^2}{d^2}+\frac{h^3}{d^3}=0, \tag{3.8}$$

with the partial derivatives

$$F_h=\frac{2\mathscr{B}}{d}(1+h'^2)^{-1/2}+\frac{(2\mathscr{F}+1-2\mathscr{B})}{d}-\frac{2(\mathscr{F}+2)h}{d^2}+\frac{3h^2}{d^3} \tag{3.9}$$

and

$$F_{h'}=\frac{2\mathscr{F}h'}{3}-2\mathscr{B}h'\frac{h}{d}(1+h'^2)^{-3/2}. \tag{3.10}$$

These derivatives always exist and are bounded. However, we can have $F_{h'}=0$, so singular points may exist. They are investigated in the following sections.

(b) Limiting cases for solitary waves

We consider here several limiting cases of equation (3.8) which deserve a particular attention.

(i) Pure gravity waves

For pure gravity waves $\mathscr{B}=0$, letting $\mathscr{F}=1+a/d$, the solitary wave solution is

$$h=d+a\,\mathrm{sech}^2\left(\frac{\kappa x}{2}\right) \quad \text{and} \quad (\kappa d)^2=\frac{3a}{(d+a)},$$

which is explicit and well-known since the work of Serre [15]. Note that a should be non-negative.

(ii) Pure capillary waves

Pure capillary waves are obtained when $g=0$ that is letting $\mathscr{F}\to\infty$ and $\mathscr{B}\to\infty$ but keeping $\mathscr{W}$ constant. Equation (3.8) divided by $\mathscr{F}$ then becomes

$$F(h',h)\equiv\frac{h'^2}{3}+\frac{2\mathscr{W}h/d}{(1+h'^2)^{1/2}}-1+\frac{2(1-\mathscr{W})h}{d}-\frac{h^2}{d^2}=0. \tag{3.11}$$

Equation (3.11) is still cubic in $(1+h'^2)^{1/2}$ but only quadratic in h.

Clearly, F vanishes at the point $h=d$, $h'=0$. The Taylor expansion near $h=d$, $h'=0$ at order 4 (i.e. near $x=\pm\infty$) gives

$$F(h',h)\approx(\tfrac{1}{3}-\mathscr{W})h'^2-(h-d)^2-\mathscr{W}(h-d)h'^2+(\tfrac{3}{4})\mathscr{W}h'^4, \tag{3.12}$$

that is a quadratic equation in h'^2. So for $\mathscr{W}>\frac{1}{3}$, the only solution starting at $(h=d,h'=0)$ is the constant solution $h=d$. For values $\mathscr{W}\leqslant\frac{1}{3}$, because $F(0,h)=-(h/d-1)^2$, as we shall see below, there are no regular solitary waves. In 3*b*(iii), we shall introduce singular solutions which correspond to angular solitary waves (*peakons*) with zero semi-curvatures. However, it can be shown that for pure capillary equations, there are no such singular solutions.

(iii) Approximation for small slopes

Assuming that $|h'|\ll 1$, one can reasonably use the approximation

$$(1+h'^2)^{-1/2}\approx 1-\tfrac{1}{2}h'^2$$

and equation (3.8) becomes

$$\left(\frac{\mathscr{F}}{3}-\frac{\mathscr{B}h}{d}\right)h'^2\approx\mathscr{F}-\frac{(2\mathscr{F}+1)h}{d}+\frac{(\mathscr{F}+2)h^2}{d^2}-\frac{h^3}{d^3}. \tag{3.13}$$

The solutions of this equation can be obtained analytically, as for pure gravity waves. Indeed, with the change of independent variable

$$\mathrm{d}\xi=\left|1-\frac{3\mathscr{W}h}{d}\right|^{-1/2}\mathrm{d}x,$$

equation (3.13) yields

$$\frac{\mathscr{F}}{3}\left(\frac{\mathrm{d}h}{\mathrm{d}\xi}\right)^2=\mathscr{F}-\frac{(2\mathscr{F}+1)h}{d}+\frac{(\mathscr{F}+2)h^2}{d^2}-\frac{h^3}{d^3},$$

that can be explicitly solved

$$h(\xi)=d+a\,\mathrm{sech}^2\left(\frac{\kappa\xi}{2}\right), \quad (\kappa d)^2=\frac{3a}{(d+a)} \quad \text{and} \quad \mathscr{F}=1+\frac{a}{d},$$

and $x(\xi)$ can be also obtained explicitly as a complicated expression (not given here as it is secondary for the purpose of this paper).

(c) Regular waves

For regular waves, the crest at $x=0$ is smooth with $h'(0)=0$ and $h(0)=d+a$, a being the wave amplitude (not necessarily positive). Equation (3.8) then yields

$$\mathscr{F}=1+\frac{a}{d},$$

thence the amplitude is independent of the Bond number $\mathscr{B}$.

(d) Asymptotic analysis

For solitary waves decaying exponentially in the far field, we have $h\sim d+a\exp(-\kappa x)$ as $x\to+\infty$, where κ is a trend parameter such as $\mathrm{Re}(\kappa)>0$. Equation (3.8) then yields the relation

$$\mathscr{F}=\frac{3-3\mathscr{B}(\kappa d)^2}{3-(\kappa d)^2}\quad\text{or}\quad(\kappa d)^2(\mathscr{F}-3\mathscr{B})=3(\mathscr{F}-1). \tag{3.14}$$

Because $\mathscr{F}$ and $\mathscr{B}$ are both real numbers, this relation shows that κ should be either real or pure imaginary, i.e. there are no solitary waves with damped oscillations (and with exponential decay). The special case $\mathscr{B}=\frac{1}{3}$ yields $\mathscr{F}=1$ or $\kappa d=\sqrt{3}$. Higher-order terms (not given here) then show that $\mathscr{F}=1$ and $\kappa d=\sqrt{3}$. Conversely, the special case $\mathscr{F}=1$ yields $\mathscr{B}=\frac{1}{3}$ and κd is undefined from the relation (3.14), but higher terms give $\kappa d=\sqrt{3}$. Possible solutions of this type are investigated in the §4 below.

For solitary waves decaying algebraically in the far field, we have $h\sim d+a(\kappa x)^{-\alpha}$ as $x\to+\infty$, where $\alpha>1$ is a parameter. Equation (3.5) then yields, necessarily, that $\mathscr{F}=1$. Thus, if algebraic solution exist, then they must occur at the critical Froude number. Considering higher-order terms (not given here), integer values of $\alpha>2$ suggest that we should have $\mathscr{B}=\frac{1}{3}$. For $\alpha=2$, similar consideration suggests that there may be algebraic solitary waves when $\mathscr{B}\neq\frac{1}{3}$.

The asymptotic analysis provides only partial information. The techniques of the phase space analysis, exposed in §4, allow us to obtain more complete information on the qualitative behaviour of solutions and unveil new interesting phenomena. In particular, we shall see that algebraic solitary waves exist only as weak solutions, i.e. with an angular crest.

(e) Singular values

Singular points are such that $F_{h'}=0$. This condition leads to three real possibilities, denoting $h_0=h(0)$ and $h'_0=h'(0)$,

$$h'=h'_0\equiv 0\quad\text{and}\quad h'=h'_\pm\equiv\pm\left[\left(\frac{3\mathscr{B}h}{\mathscr{F}d}\right)^{2/3}-1\right]^{1/2}, \tag{3.15}$$

where the condition $h/d\geq\mathscr{F}/3\mathscr{B}$. The case $h'=0$ yields, from $F=0$, that $h=d$ or $h=\mathscr{F}d$.

4. Phase plane analysis for solitary waves

In this section, we apply algebraic techniques to the PPA of solitary waves. In coherence with the asymptotic analysis, we assume that when x tends to plus or minus infinity

$$h(\infty)=d\quad\text{and}\quad h'(\infty)=0. \tag{4.1}$$

Note that $h=d$ is therefore a trivial solution of our problem. Because in equation (3.8), h' only appears by its square h'^2 and $h(-\infty)=h(\infty)$, if $h(x)$ is a solution of the equation, then $h(-x)$ is also a solution. Therefore, our equation admits symmetric solutions, but the whole set of solutions is not limited to symmetric ones.

For the convenience of the reader and the clarity of the pictures, we make the following mild simplifications: we focus on the cases where $(\mathscr{F},\mathscr{B})\in[0,2]\times[-1,2]$ (in accordance with physical

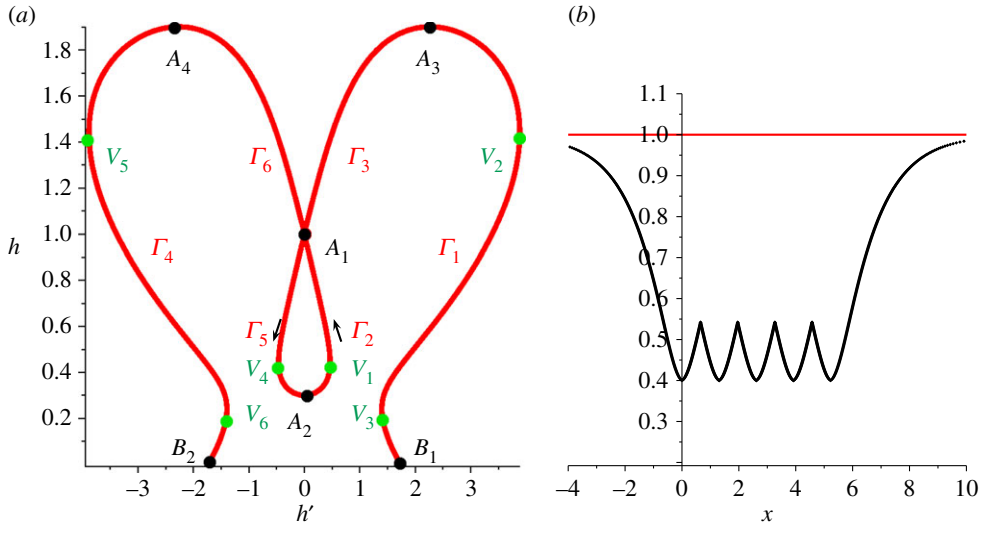

Figure 1. (*a*) Phase space diagram from §1. (*b*) Multi-angular wave. (Online version in colour.)

reasons) and, when simplification is needed, we normalize d to 1 without loss of generality. We use subscripts to indicate the parameters $(\mathscr{F},\mathscr{B})$ and omit them when there are no ambiguities.

To explain our approach, let us note that our generalization of the SGN equation takes into account gravity, inertia and capillarity. The balance between the effects of the former- is expressed by the parameter $\mathscr{F}$: when $\mathscr{F}>1$, the kinematic energy dominates the potential energy, correlatively, the solitary waves will be of elevation, whereas when $\mathscr{F}<1$, the solitary wave is of depression. Similarly, the balance between the effects of capillarity and gravity (resp. inertia) is expressed by the parameter $\mathscr{B}$ (resp. $\mathscr{W}$), but now the transition appear when $\mathscr{B}=\frac{1}{3}$ (resp. $\mathscr{W}=\frac{1}{3}$). To these different effects (hence behaviours of the solutions) is associated a first rough partition of the parametric plane $(\mathscr{F},\mathscr{B})$, delimited by the three lines $\mathscr{F}=1$, $\mathscr{B}=\frac{1}{3}$ and $\mathscr{F}=3\mathscr{B}$. We aim to refine this partition, by considering additional curves in the parametric plane, in order to classify all the possible appearances of solitary waves.

In order to discuss the number and behaviour of the solutions of the differential equation $F_{\mathscr{F},\mathscr{B}}(h',h)=0$, with respect to the pair of parameters $(\mathscr{F},\mathscr{B})\in[0,2]\times[-1,2]$, our approach is to describe graphically the variations of h and h', through the corresponding family of real algebraic curves $C_{\mathscr{F},\mathscr{B}}\in\mathbb{R}^2$. The implicit equation of $C_{\mathscr{F},\mathscr{B}}$ is $F_{\mathscr{F},\mathscr{B}}(h',h)=0$. We will decompose the parameters space $(\mathscr{F},\mathscr{B})$, with our restriction to the rectangle $[0,2]\times[-1,2]$, into subdomains where the plane curves $C_{\mathscr{F},\mathscr{B}}$ have the same 'shape' (in particular the same topology). Some subdomains can be very small, so to overcome the resulting computational difficulties, the study of the curves delimiting the subdomains will be performed with certified topology methods (e.g. [16,17] and the references therein).

(a) An example of phase diagram

Let us illustrate our approach with the phase plane description for some value of the parameters, for instance, $\mathscr{F}=0.3<1$ and $\mathscr{B}=0.8>\frac{1}{3}$. The corresponding curve $C_{0.3,0.8}$ is shown in figure 1*a*. Because the values 0.3 and 0.8 are exact rational numbers, they can be plotted simply relying on a discretization, e.g. with Matlab or drawn with a certified topology technique using specialized programs such as the algebraic curves package MAPLE or AXEL (see http://axel.inria.fr). In particular, this means that loops of whatever size are preliminary detected relying on exact (given certain precision) numerical and algebraic computations. Note that the curve is symmetric with

respect to the h-axis. This geometric property is general in our model, because the equations involve only the square of the derivative h'.

After computing the points of the curve with a horizontal tangent and the singular points, we can decompose the curve into a finite number N of graphs portions Γ_j, $j=1,\dots,N$ of type $h'=\phi_j(h)$, for some differentiable functions ϕ_j, $j=1,\dots,N$ according to the implicit function theorem. The endpoints of each graph correspond to critical points of the (horizontal) projection of the curve on the h-axis. The points with a horizontal tangent or multiple points satisfy the additional explicit condition $\partial_{h'}F=0$. On every graph, we have an explicit (possibly nonlinear) ODE $\mathrm{d}x=\mathrm{d}h/\phi_j(h)$ which can be integrated by standard techniques. Moreover, where h' is positive (resp. negative), h should increase (resp. decrease), so each Γ_j can be oriented (see figure 1 where the curve can be decomposed into $N=6$ oriented curve segments).

In this particular example, there are four points on the curve such that $\partial F/\partial h'=0$: $A_1=(0,1)$, $A_2=(0,0.3)$, $A_3\approx(2,1.9)$ and $A_4\approx(-2,1.9)$. Call B_1 and B_2 the intersections of the curve with the h' axis. Then, we get the following going up branches: Γ_1 from B_1 to A_3, Γ_2 from A_2 to A_1 (on the right side) and Γ_3 from A_1 to A_3. Symmetrically, the downgoing branches Γ_j for $j=\{4,5,6\}$ are in the left half-plane $h'<0$.

Constrained by the asymptotic conditions (4.1), we consider only homoclinic paths starting from A_1 and arriving at A_1. Topologically, they correspond to loops. In this example, the only continuous such loop is going down on Γ_5 from A_1 to A_2 (on the left side), then going up on Γ_2 from A_2 to A_1 (on the right side). It will correspond to the unique differentiable solution $h(x)$ of the differential equation.

Inspired by the examples computed by Stokes [2] and by the analysis of the 'peakons' of some nonlinear dispersive equations such as the Camassa–Holm, Degasperis–Procesi and other equations [4,9,10,18], we also consider a different class of solutions, which are sometimes referred to as *singular solutions* in the classical literature [8,19,20]. Here, they correspond to solitary waves with one (or several) angular points. However, because there are an infinity of angular solutions, we additionally require that the two semi-derivatives of $h(x)$ at the angle are opposite in sign and that the two second semi-derivatives vanish. This property was put in evidence by Stokes in his limiting wave construction. Physically, this means that the wave is symmetric at the crest and that the fluid vertical acceleration is zero at the crest.

In total, there are six points on the curve $C_{0.3,0.8}$ with a vertical tangent line. They have approximately the following coordinates: $V_1=(0.5,0.4)$, $V_2=(4,1.4)$ $V_3=(1.3,0.2)$ and their symmetric counterparts, V_4, V_5 and V_6, with respect to the h-axis. The two semi-second derivatives at these points are zero. On the one hand, two points V_2 and V_3, and their symmetric counterparts, belong to graphs not connected to A_1. On the other hand, V_1 and V_4 are connected to A_1, respectively, by the Γ_2 and Γ_5 branches. So, we can form a discontinuous symmetrical loop going down from A_1 to V_4 (on Γ_5), jumping from V_4 to V_1, then going up from V_1 to A_1 (on Γ_1). It corresponds to a new solitary wave with an angular point, a so-called *peakon*, $h(x)$ satisfying all the conservation laws. We can consider as well another loop going down from A_1 to A_2 (on the left side), then going up from A_2 to V_1 (on the right side), then jumping from V_1 to V_4, and cycling through V_4, A_2, V_1, V_4, then finally going up from A_2 to the boundary point A_1. The corresponding solution has a finite number of 'peaks' (figure 1*b*). The angular points are emphasized in figure 1*b* by green solid discs.

Additionally, one can construct a discontinuous path going from A_1 to A_3, jumping to A_4 and going back to A_1. This will correspond to a singular solitary wave with a cusp at the crest. However, such solutions should be discarded based on physical considerations, because it leads to infinite accelerations in the singularity point.

We now aim to generalize the analysis given above for $\mathscr{F}=0.3$ and $\mathscr{B}=0.8$ to all pairs $(\mathscr{F},\mathscr{B})\in[0,2]\times[-1,2]$. Clearly, for a very small perturbation $\mathscr{F}=0.3+\epsilon_1$ and $\mathscr{B}=0.8+\epsilon_2$, the curves remain qualitatively very similar. In fact, one can pass from the curve $C_{0.3,0.8}$ to $C_{0.3+\epsilon_1,0.8+\epsilon_2}$ by a homotopy respecting the decomposition in oriented graphs we have described. However, for larger perturbations of $\mathscr{F}$ and $\mathscr{B}$ numbers, we may have qualitatively different curves and results. For instance, under a deformation, the considered loop retracts to one point

and disappears completely; so do solitary wave solutions described above. This abrupt change of behaviour is usually called a bifurcation. In our application, the bifurcations may occur when one of the numbers of special points (multiple point, point with a vertical or a horizontal tangent) of the curve $C_{\mathscr{F},\mathscr{B}}$ changes.

Our purpose is to describe all possible situations (up to qualitative similarity) and to delimit the corresponding parameters $(\mathscr{F},\mathscr{B})$ ranges. Owing to the algebraic nature of the problem, these regions are organized in a finite number of semi-algebraic sets, i.e. the equations of their borders are polynomials in $(\mathscr{F},\mathscr{B})$ that can be effectively computed. On the borders of the open domains, we will also have special extremal behaviours, which are described below.

(b) Local analysis where $h' = 0$

The points on the h-axis are important because they correspond to the wave crest or trough. To determine them, it is sufficient to substitute $h' = 0$ and solve the resulting equation in h $F_{\mathscr{F},\mathscr{B}}(0,h) = 0$, that gives either $h = d$ with multiplicity 2, or $h = d\mathscr{F}$. If there is a branch of type Γ connecting these two points, then there should be also the symmetric one. Consequently, we can consider the path starting from $A_1 = (h' = 0, h = d)$ and going up (resp. down) to $A_2 = (h' = 0, h = d\mathscr{F})$ if $\mathscr{F} > 1$ (resp. $\mathscr{F} < 1$); and then back from A_2 to A_1. This could correspond to the crest (trough) of a solitary wave, above (below) the still water level $h = d$.

Then, in order to investigate the local behaviour at $A_1 = (h' = 0, h = d)$, we compute the Taylor expansion of F at this point. It is similar to the asymptotic analysis conducted in §3d. By expanding the equation to the second order, we obtain

$$d^2(\mathscr{F} - 3\mathscr{B})h'^2 - 3(\mathscr{F} - 1)(h - d)^2 = 0 + \mathrm{O}((h - d)^3, h'^4).$$

There are three distinct cases to consider depending on the sign of the expression $(\mathscr{F} - 1)(\mathscr{F} - 3\mathscr{B})$:

— if $(\mathscr{F} - 1)(\mathscr{F} - 3\mathscr{B}) < 0$, A_1 is an isolated point of the curve $C_{\mathscr{F},\mathscr{B}}$. This implies that the only solution is the trivial one $h = d$.
— if $(\mathscr{F} - 1)(\mathscr{F} - 3\mathscr{B}) > 0$, A_1 is a double point corresponding to the crossing of two branches of $C_{\mathscr{F},\mathscr{B}}$. Hence, there is no obstruction (at least at the level of this local analysis) for the existence of a solitary wave.
— if $(\mathscr{F} - 1)(\mathscr{F} - 3\mathscr{B}) = 0$, with $\mathscr{F} = 1$. Then, $A_1 = A_2$ and we must consider the Taylor expansion up to the third order

$$d^3(1 - 3\mathscr{B})h'^2 + 3(h - d)^3 - d^2(h - d)h'^2 = 0. \tag{4.2}$$

Therefore, if $\mathscr{B} > \frac{1}{3}$ (resp. $\mathscr{B} < \frac{1}{3}$), the curve $C_{\mathscr{F},\mathscr{B}}$ admits at A_1 a cusp above (resp. below) A_1. While in the case $\mathscr{B} = \frac{1}{3}$, the Taylor expansion corresponds to three smooth branches including $h = d$. As a consequence, there is no obstruction (in this local analysis) for the existence of a solitary wave solution with an angular point (i.e. a peakon).
— if $(\mathscr{F} - 1)(\mathscr{F} - 3\mathscr{B}) = 0$, with $\mathscr{F} = 3\mathscr{B}$ and $\mathscr{F} \neq 1$. In this case, the Taylor expansion to the third order is

$$(h - d)[(3\mathscr{B} - 1)(h - d) - \mathscr{B}d^2h'^2 = 0,$$

that gives locally a line $(h = d)$ and a smooth curve (a parabola). As a consequence, there is no obstruction for the existence of a non-trivial solitary wave solution with an angular point and an algebraic decrease at infinity.

Now, we perform a similar local analysis for the point A_2. The Taylor expansion to the second order of the equation $F(h', h) = 0$ at the point $A_2 = (h' = 0, h = d\mathscr{F})$, yields

$$3(\mathscr{F} - 1)^2(h - d\mathscr{F}) = d\mathscr{F}(3\mathscr{B} - 1)h'^2.$$

Thus, when $\mathscr{F} \neq 1$ and $\mathscr{B} \neq \frac{1}{3}$, we obtain a regular point with a horizontal tangent. It is of convex type if $\mathscr{B} > \frac{1}{3}$ and concave if $\mathscr{B} < \frac{1}{3}$. Therefore, if $\mathscr{F} < 1$ and $\mathscr{B} > \frac{1}{3}$, or if $\mathscr{F} > 1$ and $\mathscr{B} < \frac{1}{3}$, then

there is no obstruction for the existence of a solitary wave. While if $\mathscr{F} < 3\mathscr{B} < 1$ or if $\mathscr{F} > 3\mathscr{B} > 1$, this local analysis allows only an angular solitary wave.

When $\mathscr{F} \neq 1$ and $\mathscr{B} = \frac{1}{3}$, the Taylor expansion of the equation at the point A_2 yields

$$\mathscr{F} h'^4 \sim 4(\mathscr{F} - 1)^2 (h - d).$$

In other words, the curve has a flat point (the curvature vanishes).

As a main conclusion of this local analysis, the parameter plane $(\mathscr{F}, \mathscr{B})$ is partitioned into six regions delimited by the three straight lines $\mathscr{F} = 1$, $\mathscr{B} = \frac{1}{3}$ and $\mathscr{F} = 3\mathscr{B}$. We would like to underline that these lines correspond to critical physical regimes.

(c) Local analysis where $h' \neq 0$

As noted in the end of §4a, a solitary wave is associated with a path on the curve $C_{\mathscr{F},\mathscr{B}}$ from the point $A_1 = (0, 1)$ to a point with a horizontal or vertical tangent. Therefore, these points play a key role in our analysis.

(i) Local analysis in points with a horizontal tangent

These points satisfy the system of two equations $F(h', h) = 0$ and $\partial_{h'} F(h', h) = 0$. For $h' \neq 0$, the second equation is satisfied when $d^2 \mathscr{F}^2 (1 + h'^2)^3 = (3\mathscr{B} h)^2$. From the last expression, we find h'^2 as a function of h and replace it in the equation $F = 0$. Thus, we obtain a nonlinear equation depending only on h, but involving a cubic root operator. To get rid of this irrational function and deal only with polynomials, we introduce a new variable Y such that $h = (d\mathscr{F}/3\mathscr{B})Y^3$. Thence, $h'^2 = Y^2 - 1$, with $Y \geq 1$. Eventually, we obtain the following polynomial equation of degree nine in Y whose coefficients are polynomial functions of $\mathscr{F}$ and $\mathscr{B}$

$$f(Y) \equiv \mathscr{F}^2 Y^9 - (3\mathscr{F} - 2)\mathscr{F}\mathscr{B} Y^6 + 9\mathscr{B}^2 (1 + 2\mathscr{F} - 2\mathscr{B}) Y^3 + 27\mathscr{B}^3 Y^2 - 36\mathscr{B}^3 = 0. \tag{4.3}$$

The appropriate tool to discuss the number of real roots of $f(Y)$ is the discriminant $D_1(\mathscr{F}, \mathscr{B})$, which is a polynomial function in the variables $(\mathscr{F}, \mathscr{B})$ and it generalizes the well-known discriminant of a quadratic equation in Y. The zero level set of D_1 is an algebraic curve $\mathscr{D}_1$ in the $(\mathscr{F}, \mathscr{B})$-plane. It characterizes the values of $(\mathscr{F}, \mathscr{B})$, where $f(Y)$ experiences the collision of (real or complex) roots. For the algebraic definition and first properties of the discriminant see, e.g. [21] or chapter 5 of the classical textbook [22]. For multidimensional extensions, we refer to reference [23]. The key property of our analysis is that the curve defined by the implicit equation $D_1(\mathscr{F}, \mathscr{B}) = 0$ divides the parametric $(\mathscr{F}, \mathscr{B})$-plane into domains where $f(Y)$ has the same number of real roots. However, we would like to make the important observation that some branches of the discriminant locus $\mathscr{D}_1$ correspond to the collision of complex roots of $f(Y) = 0$, without any visible effects on the real roots. In this case, these two domains have to be merged into a single one. These situations require a special post-processing procedure.

By definition of the Y variable, its values of physical interest are necessarily greater or equal than one. Thus, the subdomains of the $(\mathscr{F}, \mathscr{B})$-plane where the additional condition $Y \geq 1$ is fulfilled by real roots are delimited by some ovals of the zero level-set $f_{\mathscr{F},\mathscr{B}}(1) = 0$. As above, it is possible that the zero level-set contains parasitic ovals which do not lead to any visible effects on the real roots, when one crosses their boundary. Eventually, we construct explicitly a partition of the rectangle $[0, 2] \times [-1, 2]$ into connected domains. In each cell, the number of local extrema of h on $C_{\mathscr{F},\mathscr{B}}$ is constant.

(ii) Local analysis in points with a vertical tangent

We follow the same methodology already employed above to study the points of the curves $C_{(\mathscr{F},\mathscr{B})}$ with a vertical tangent. They satisfy the system of two equations $F = 0$ and $\partial_h F = 0$.

Computing $F(h,h') - h\partial_h F$, we eliminate the irrational terms. By introducing a new variable Z such that $h'^2 = Z^2 - 1$, we arrive to the equation

$$\mathscr{F}(Z^2-1) = -3\left(\frac{h}{d}-1\right)\left(2\left(\frac{h}{d}\right)^2 + \frac{\mathscr{F}h}{d} + \mathscr{F}\right). \tag{4.4}$$

We can also replace h'^2 by $Z^2 - 1$ in the irrational equation $F(h,h') = 0$ to obtain a new polynomial equation $G(h,Z) = 0$. Because now we are left with two polynomial equations (4.4) and $G(h,Z) = 0$ for the variables (h,Z), we can eliminate h computing their resultant with respect to h. Thus, we obtain a polynomial $g_{\mathscr{F},\mathscr{B}}(Z)$ of degree six in Z, which plays the same role that the polynomial $f_{\mathscr{F},\mathscr{B}}(Y)$ in the previous section. Similarly, we compute the discriminant of the polynomial of g with respect to the variable Z to find a polynomial expression $D_2(\mathscr{F},\mathscr{B})$. As explained above, it allows to decompose the parameters space $(\mathscr{F},\mathscr{B})$ into cells where the number of points on the curve with a vertical tangent is the same. We also require that these points satisfy an additional condition $h > 0$, which physically means the absence of dry areas.

Finally, we take the intersection of two families of cells we constructed in this section. As a result, we construct explicitly a cell decomposition of the rectangle $[0,2] \times [-1,2]$. In each cell, the numbers of local extrema of h and h' on $C_{\mathscr{F},\mathscr{B}}$ are preserved. Hence, we are able to classify all possible shapes of $C_{\mathscr{F},\mathscr{B}}$ with respect to admissible paths connecting A_1 either to a point with $h' = 0$ or to a point with a vertical tangent.

(d) Partition with a fixed parameter

Here, we describe the deformation of the curves when they undergo the continuous parameters change. For the sake of simplicity, we fix one parameter (say $\mathscr{B} = 0.32$) and vary the other one. The Froude number $\mathscr{F}$ will take the values in the segment $[0, 2.5]$ to produce a continuous family of curves $C_{\mathscr{F},0.32}$. As expected, the shape of the curves changes only for special values of the parameter $\mathscr{F}$. Thus, we obtain a decomposition of the segment $[0, 2.5]$ into a finite numbers of intervals where the shape is maintained. Below, we consider several typical behaviours. Keeping the notation of the previous section, we conduct the computations.

The discriminant $D_1(\mathscr{F}, 0.32)$ has four real roots, which are equal (approximately) to -8.0793, 0, 0.96, 0.966423. In this list, we can recognize the two special values already detected above, i.e. $\mathscr{F} = 0$ and $\mathscr{F} = 3\mathscr{B} = 0.96$. The value $\mathscr{F} = -8.0793$ is outside the interval of physical interest. The discriminant $D_2(\mathscr{F})$ has six real roots, equal approximately to -8.8226, -8.0793, 0, 0.95678, 0.966423, 2.0382. Again, we recognize the special value $\mathscr{F} = 0$ along with two previously detected roots of $D_1(\mathscr{F}, 0.32)$. Moreover, we obtain a new value $\mathscr{F} = 0.95678$, whereas the value of $\mathscr{F} = -8.8226$ is outside of the considered interval. During the local asymptotic analysis around the points where $h' = 0$, we discarded the segment delimited by $(\mathscr{F} - 1)(\mathscr{F} - 3\mathscr{B}) < 0$, which corresponds to $[0.96, 1]$ in the present case. Finally, we have to analyse only the segments: $[0, 0.95678]$, $[0.95678, 0.96]$, $[1, 2.0382]$ and $[2.0382, 2.5]$ along with their endpoints.

For each segment, it is sufficient to choose only one value for $\mathscr{F}$ (inside this interval) and plot the corresponding curve $C_{\mathscr{F},0.32}$. Here, we summarize our main findings.

(i) For $\mathscr{F} = 0$, there are neither vertical nor horizontal tangents. Therefore, there are no non-trivial solutions.
(ii) For $\mathscr{F}$ strictly between 0 and 0.95678, there are points with vertical as well as horizontal tangents to the curve, but their relative locations, with respect to the orientation, do not allow the existence of an admissible non-trivial solitary wave. See figure 2*a* for an illustration.
(iii) The value of $\mathscr{F} = 0.95678$ corresponds to the collision of complex roots and it does not bring anything for the real curve. Consequently, this boundary point has to be removed from the present discussion.
(iv) For $\mathscr{F} = 0.96$, which is a special value because $\mathscr{F} = 3\mathscr{B} = 0.96$, there is only one admissible path to the point with a vertical tangent; see figure 2*b* for the illustration.

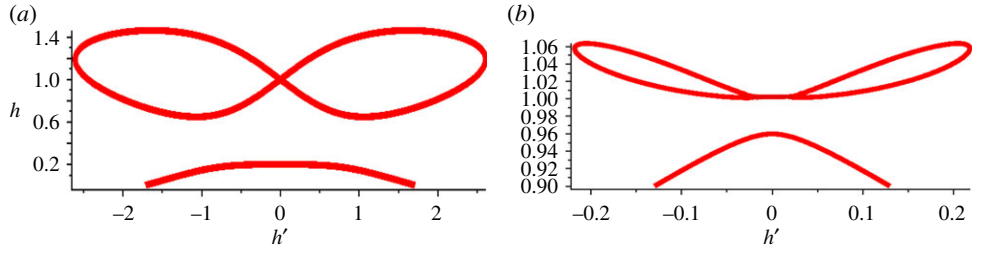

Figure 2. Algebraic curve in the phase space (*a*) $C_{0.2,0.32}$ and (*b*) $C_{0.96,0.32}$. (Online version in colour.)

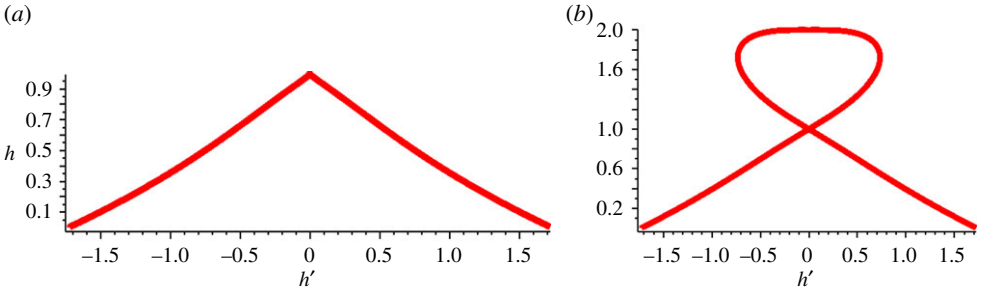

Figure 3. Algebraic curve in the phase space (*a*) $C_{1,0.32}$ and (*b*) $C_{2,0.32}$. (Online version in colour.)

It corresponds to a single peakon-like wave. It has an additional interesting property, because it decreases only algebraically to infinity (all other solutions considered herein above had an exponential decay).

(v) For $\mathscr{F}$ lying strictly between 0.96 and 1, as noted earlier, there are only one isolated point at $(h=1, h'=0)$. Therefore, there are no non-trivial solutions.

(vi) For $\mathscr{F}=1$, which is also a special critical value, the curve $C_{1,0.32}$ admits a cusp at $(h=1, h'=0)$, and there are neither vertical nor horizontal tangents. Therefore, there are no non-trivial solutions in this case (figure 3*a*).

(vii) For $\mathscr{F}$ strictly greater than 1 and smaller than 2.0382, there are points with a vertical as well as horizontal tangents to the curve $C_{\mathscr{F},0.32}$ (figure 3*b*). Note that the loop of this curve resembles the one analysed in our first example of §4a. The only difference consists in the loop orientation (upward). So, for this range of values, there is a regular solitary wave with a smooth crest. By including discontinuous patches, we can also construct admissible peakons with a finite number of crests, as illustrated in figure 1*b*.

(viii) The value of $\mathscr{F}=2.0382$ is not relevant for our discussion.

(e) Types of behaviours

For our final classification, it is worthwhile to give names to the different kind of qualitative behaviours we already encountered. Let us denote by a 0, *I*, *II*, the types which appear generically (on open subdomains of the parameters space), and by E_1, E_2, E_3 the more extreme types which appear on the discriminants components (lines or curves). So, let us call

— type 0, the kind of situation, like in the first or second previous items, where no regular or generalized solitary wave may occur, besides the trivial one $h=d$;
— type I, the kind of situation, like in example 1, where there are a regular wave with a trough and also generalized peakon solutions with one or several angles;
— type II, the kind of situation, like in the previous item (vii), where there are a regular wave with a crest and also generalized peakon-like solutions with one or several angles;

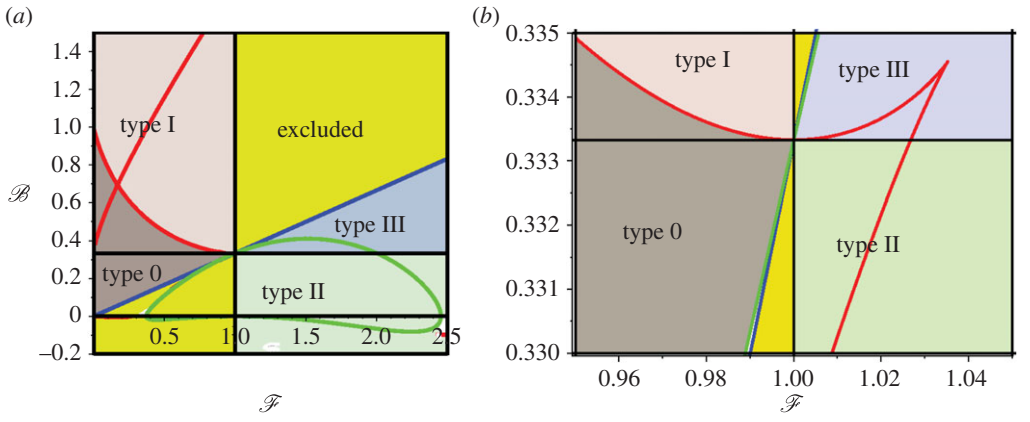

Figure 4. (*a*) Discriminant loci and (*b*) a zoom on region around the point $(1, \frac{1}{3})$. (Online version in colour.)

In addition, let us name the first kind of extremal situation we already encountered

— type E_1, the kind of situation, as in the third previous item, $\mathscr{F} = 3\mathscr{B}$, but $\mathscr{F} \neq 1$, with a single peakon, i.e. it admits a symmetric single angular solitary wave. It also has an algebraically decrease to infinity.

We will see that the very extremal case $\mathscr{F} = 3\mathscr{B}$ and $\mathscr{F} = 1$, admits the same type of solutions.

(f) Configuration space partition

In this section, we consider both the parameters $(\mathscr{F}, \mathscr{B})$ as variables which are free to take any values from the rectangle $[0, 2] \times [-1, 2]$. Our aim is to construct a cellular decomposition of this domain, each cell containing a different type of behaviour of the solution. For this purpose, we employ the computer algebra system MAPLE. More specifically, using MAPLE commands *discrim*() and *factor*(), we can show that the discriminant polynomial D_1 can be decomposed into the product of a square $(\mathscr{F} - 3\mathscr{B})^2$ and another polynomial of degree 10 that we denote by $D(\mathscr{F}, \mathscr{B})$. The zero locus of D (shown in red) together with the special lines $\mathscr{B} = \frac{1}{3}$, $\mathscr{B} = \mathscr{F}/3$ and $\mathscr{F} = 1$ are shown in figure 4. A zoom on a region of interest around $\mathscr{B} = \frac{1}{3}$ and $\mathscr{F} = 1$ is provided in figure 4*b*.

Similarly, we decompose the other discriminant polynomial $D_2(\mathscr{F}, \mathscr{B})$. As a result, we find the product of the same polynomial $D(\mathscr{F}, \mathscr{B})$ by powers of $\mathscr{F}$, powers of $\mathscr{B}$ and by the cube of another polynomial that we denote by $D_3(\mathscr{F}, \mathscr{B})$. The zero locus of $D_3(\mathscr{F}, \mathscr{B})$ is shown in green in figure 4.

Figure 4 shows only a preliminary partition of the area under consideration. As it was illustrated in the previous section on a simple one-dimensional example (with the variable $\mathscr{F}$ number), some boundaries are artificial in the real domain. Consequently, in the following, we analyse separately each case.

The line in the parameters plane and defined by the linear relation $\mathscr{F} = 3\mathscr{B}$ gives rise to a double root at a fixed value $Y = 1$. In other words, it is the double point at $h = 1$ and $h' = 0$.

(i) Additional types and classification

Considering each of the delimited domains, allow to classify all the possible curves $C_{\mathscr{F},\mathscr{B}}$, by the relative location of their points with horizontal tangent, vertical tangent, singularity. For each such type of curve, we analysed all the possible admissible paths (with respect to the orientation) departing from $A_1 =$ and arriving to a point with a vertical tangent, or to a point of the line $h' = 0$. To each of them, a regular or an angular solitary wave is associated.

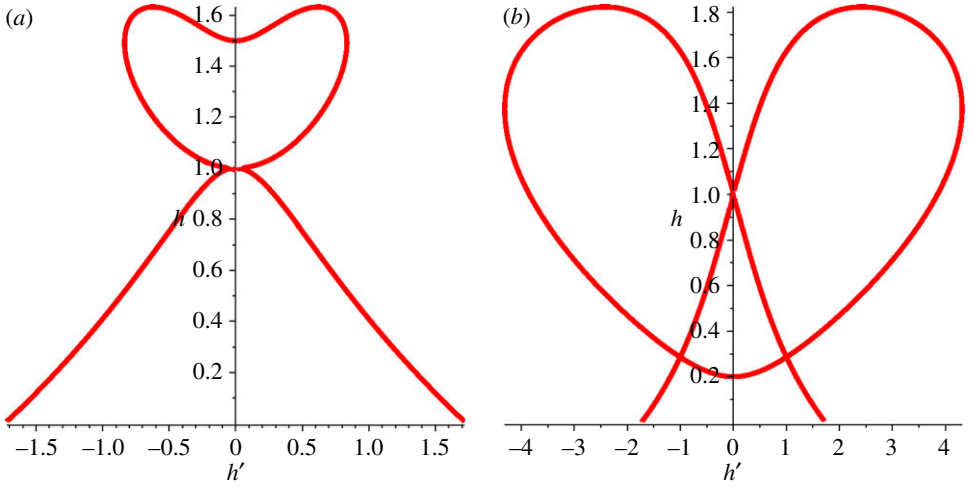

Figure 5. (*a*) A semi-extremal and extremal (*b*) curves. (Online version in colour.)

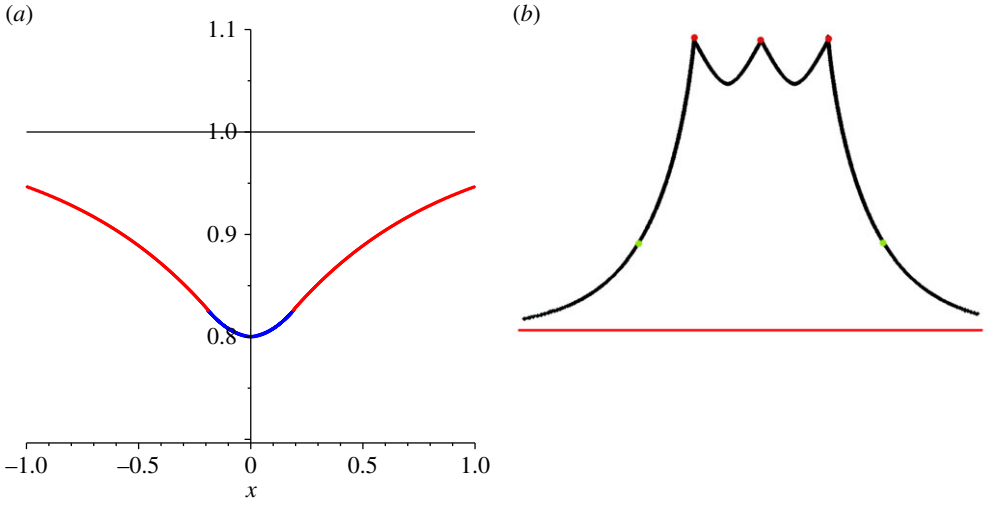

Figure 6. (*a*) A weakly regular solitary wave. (*b*) A weak multi-angular crested wave. (Online version in colour.)

We found only two types of regular solitary waves: a crest when $\mathscr{F} > 1$, that we called type II, and a through when $\mathscr{F} < 1$, that we called type I. We have to introduce a new 'generic' type.

— Type III corresponds to the open subset of the parameter space with $\mathscr{F} > 1$, $\mathscr{F} > 3\mathscr{B}$ and $\mathscr{B} > 1/3$, where there are no regular wave but generalized peakon-like solutions with one angle-like illustrated in figure 5*a*.

Besides type E_1, we found the following extremal types:

— type E_2. The limiting case where $(\mathscr{F}, \mathscr{B})$ belongs to a branch of the discriminant locus, e.g. when $(\mathscr{F} = 0.2, \mathscr{B} = 0.66)$ approximately, we obtain the curve shown in figure 5*b*. There is a connected path but with an angle going from A_1 to a lower point on $h' = 0$. It gives rise to a weak regular wave shown in figure 6*a*, which has two points where the regularity is only C^1 (we represented them by changing the colours of the branches). Weakly regular periodic waves have been recently reported in [24] for some integrable equations;

— type E_3. A tiny branch of the discriminant with $\mathscr{F} > 1$ gives rise to another interesting type of 'semi-extremal curve', e.g. $C_{1.01,0.3334121494}$, shown in figure 5*a* and corresponding to (multi-) angular weak crests (figure 6*b*). The angles are indicated with a red disc and the weak defect of regularity are indicated with a green disc. Multi-angular travelling waves were also found in a completely integrable equation [25].

5. Conclusions and future work

In this paper, we addressed the problem of constructing weak solitary wave solutions using PPA and applying algebraic geometry techniques. The method is illustrated on a weakly dispersive fully nonlinear capillary–gravity waves model equations, namely the SGN equations. These equations are not trivial but yet tractable, so the power of our approach could be illustrated.

After deriving the governing SGN system of equations, we restricted our attention to a particular case of travelling solitary wave solutions. This study contains a complete phase space analysis of all admissible solutions. Among them, we found the classical infinitely smooth solitary waves of elevation ($\mathscr{F} > 1$) and of depression ($\mathscr{F} < 1$). However, by taking into consideration the discontinuous paths on the phase curves, we were able to construct peakon-like solitary waves with angular points at the crests (resp. the troughs). These 'peakons' are valid mathematical solutions to the ODE describing steady waves. Consequently, this work can be considered as a continuation of previous important studies on peaked travelling waves in some shallow water model equations (e.g. Camassa–Holm). We are aware that these solutions are of little physical applicability, because the model is pushed towards its limits. (The smooth weak solution of figure 6*a* may be physically sound, however.) Nevertheless, we believe that this work can suggest directions for improving the model. Also, singular (i.e. angular) solutions of fluid flows in the presence of surface tension exist physically [26], so our analysis could be applied to model and study these phenomena.

We reduced the characterization and classification of all admissible solutions (regular or peakon-like solitary waves) to a geometric problem. Namely, for each value of a pair $(\mathscr{F}, \mathscr{B}) \in [0, 2] \times [-1, 2]$, we found if it exists on the curve $C_{(\mathscr{F},\mathscr{B})}$, an 'admissible' path starting and ending at the point A_1 (corresponding to $h' = 0, h = d$, a boundary condition satisfied by solitons). Our strategy to solve this geometric problem was to first provide a complete classification of possible phase curve topologies using some advanced computer algebra techniques, and then discard phenomena owing to branches not connected to A_1. The algebraic methods were explained here in detail with illustrative examples. This study is a successful example of the application of some methods of effective algebraic geometry to the qualitative analysis of ODEs stemming from fluid mechanics problems. Despite the purely mathematical interest, we were able also to find some new types of solitary waves. For example, one can mention the weakly singular solitary wave (with a jump in the second derivative) along with the wave decaying algebraically at the infinity. The existence of weakly singular periodic solutions was recently hinted in an integrable model [24]. However, in our study, it is reported for the first time in an equation stemming directly from the water wave theory.

With our analysis, we pushed the SGN model towards its limits, because the Laplace capillarity law does not apply when the derivatives of the elevation jumps at a peak. Nevertheless, one observes that when we zoom out some regular sharp profile of a solitary wave, it looks like a peakon. Then, for a fixed pair of parameters $(\mathscr{F}, \mathscr{B})$, because we deal with an approximate model, we can interpret such a peakon solution as a warning: a sign for the possible existence of some sharp regular solitary wave of the exact model, with a nearby pair of parameters. This argument is emphasized when the phase plane curve corresponding to a peak is similar to a phase plane giving rise to a regular solitary wave; for example, for the curves of type III (in our classification), which are deformations of curves of type II.

In future works, we first plan to study in a similar way the families of periodic travelling wave solutions. This problem is, sensibly, more complicated, because its formulation involves

two additional parameters (integration constants) depending implicitly on the solution. Thus, this problem leads us to work in four-dimensional parameter space. Second, another research direction consists of looking for an augmented shallow water model with possibly some additional physical parameters. These extra degrees of freedom would be used to represent singular solutions as a limit of smooth ones. The main motivation for this consists of the fact that it is already the case for the full Euler (limiting Stokes wave) and the Camassa–Holm-type equations.

Authors' contributions. The author names are listed in alphabetic order as they contributed equally to this work.
Competing interests. The authors have no competing interests.
Funding. The authors acknowledge the support from CNRS under the PEPS 2015 Inphyniti programme and exploratory project FARA.
Acknowledgements. D.D. thanks the hospitality of the Laboratory J. A. Dieudonné and of the University of Nice-Sophia Antipolis during his visits to Nice.

References

1. Hairer E, Wanner G. 1996 *Solving ordinary differential equations II. Stiff and differential–algebraic problems*. Springer Series in Computational Mathematics, vol. 14. Berlin, Germany: Springer.
2. Stokes GG. 1880 Supplement to a paper on the theory of oscillatory waves. *Math. Phys. Pap.* **1**, 314–326. (doi:10.1017/CBO9780511702242.016)
3. Dressler RF. 1949 Mathematical solution of the problem of roll-waves in inclined opel channels. *Commun. Pure Appl. Math.* **2**, 149–194. (doi:10.1002/cpa.3160020203)
4. Liao S. 2013 Two new standing solitary waves in shallow water. *Wave Motion* **50**, 785–792. (doi:10.1016/j.wavemoti.2013.02.009)
5. LeVeque RJ. 1992 *Numerical methods for conservation laws*, 2nd edn. Basel, Switzerland: Birkhäuser.
6. Mura T, Koya T. 1992 *Variational methods in mechanics*. Oxford, UK: Oxford University Press.
7. Jordan DW, Smith P. 2007 *Nonlinear ordinary differential equations: problems and solutions*, 4th edn. Oxford, UK: Oxford University Press.
8. Arnold VI. 1996 *Geometrical methods in the theory of ordinary differential equations*. New York, NY: Springer.
9. Camassa R, Holm D. 1993 An integrable shallow water equation with peaked solitons. *Phys. Rev. Lett.* **71**, 1661–1664. (doi:10.1103/PhysRevLett.71.1661)
10. Degasperis A, Procesi M. 1999 Asymptotic integrability. In *Symmetry and perturbation theory* (A Degasperis, G Gaeta), pp. 23–37. River Edge, NJ: World Scientific.
11. Serre F. 1953 Contribution à l'étude des écoulements permanents et variables dans les canaux. *La Houille blanche* **8**, 830–872. (doi:10.1051/lhb/1953058)
12. Su CH, Gardner CS. 1969 KdV equation and generalizations. Part III. Derivation of Korteweg–de Vries equation and Burgers equation. *J. Math. Phys.* **10**, 536–539. (doi:10.1063/1.1664873)
13. Green AE, Laws N, Naghdi PM. 1974 On the theory of water waves. *Proc. R. Soc. Lond. A* **338**, 43–55. (doi:10.1098/rspa.1974.0072)
14. Wu TY. 2001 A unified theory for modeling water waves. *Adv. Appl. Mech.* **37**, 1–88. (doi:10.1016/S0065-2156(00)80004-6)
15. Serre F. 1953 Contribution à l'étude des écoulements permanents et variables dans les canaux. *La Houille blanche* **8**, 374–388. (doi:10.1051/lhb/1953034)
16. Gonzalez-Vega L, Necula I. 2002 Efficient topology determination of implicitly defined algebraic plane curves. *Comput. Aided Geomet. Des.* **19**, 719–743. (doi:10.1016/S0167-8396(02)00167-X)
17. Cheng J, Lazard S, Peñaranda L, Pouget M, Rouillier F, Tsigaridas E. 2010 On the topology of real algebraic plane curves. *Math. Comput. Sci.* **4**, 113–137.
18. Liao S. 2014 Do peaked solitary water waves indeed exist? *Commun. Nonlinear Sci. Numer. Sim.* **19**, 1792–1821. (doi:10.1016/j.cnsns.2013.09.042)
19. Hamburger M. 1893 Ueber die sigularen losungen der algebraischen differenzialgleichnungen erster ordnung. *J. Reine Ang. Math.* **112**, 205–246.
20. Hubert E. 1996 The general solution of an ordinary differential equation. In *Proc. the 1996 Int. Symp. on Symbolic and algebraic computation, Zurich, Switzerland*, pp. 189–195. New York, NY: ACM.

21. Nickalls RWD, Dye RH. 1996 The geometry of the discriminant of a polynomial. *Math. Gaz.e* **80**, 279–285. (doi:10.2307/3619560)
22. Lang S. 2002 *Algebra*, vol. 211. New York, NY: Springer.
23. Gelfand IM, Kapranov MM, Zelevinsky AV. 1994 *Discriminants, resultants and multidimensional determinants*. Boston, MA: Birkhäuser.
24. Chen A, Wen S, Tang S, Huang W, Qiao Z. 2015 Effects of quadratic singular curves in integrable equations. *Stud. Appl. Math.* **134**, 24–61. (doi:10.1111/sapm.12060)
25. Qiao Z. 2006 A new integrable equation with cuspons and W/M-shape-peaks solitons. *J. Math. Phys.* **47**, 112701. (doi:10.1063/1.2365758)
26. Eggers J, Fontelos MA. 2009 The role of self-similarity in singularities of partial differential equations. *Nonlinearity* **22**, R1–R44. (doi:10.1088/0951-7715/22/1/R01)